JOURNAL OF AGRICULTURAL AND FOOD CHEMISTRY

Novel Fluorescence Detection of Free Radicals Generated in Photolysis of Fenvalerate

YUSUKE SUZUKI* AND TOSHIYUKI KATAGI

Environmental Health Science Laboratory, Sumitomo Chemical Co., Ltd., 4-2-1 Takatsukasa, Takarazuka, Hyogo 665-8555, Japan

Photoinduced decarboxylation via homolytic cleavage of the ester linkage generating two benzyl radicals being recoupled is known to be a major photolytic pathway of the insecticide fenvalerate in aqueous or organic solvents. A highly sensitive and selective fluorescence spectroscopic method was applied to detect these radicals generated under xenon lamp irradiation in organic solvents and aqueous acetonitrile solutions. The short-lived radicals were efficiently trapped by the nitroxide free radical having a primary amino group, and the resultant diamagnetic adducts were instantaneously derivatized with fluorescamine as a fluorescent probe. The highly fluorescent derivatives were successfully separated and detected by a reversed-phase high-performance liquid chromatography equipped with a fluorescence detector, and their structures were individually identified by liquid chromatography/mass spectrometry.

KEYWORDS: Fenvalerate; fluorescence; radical; fluorescamine; radical trapping

INTRODUCTION

Photochemical reactions by natural sunlight are known to be one of the most important factors determining the fate of pesticide, especially in aquatic environments. The various types of reactions proceed via excited states of the pesticide, leading to structural changes, for example, by isomerization, homolytic bond cleavage, and oxidation (*1*). As a primary excitation of the molecule partly results in the formation of many unstable free radical intermediates via bond fission, a convenient method to detect these radicals is considered to be very useful not only to understand the photodegradation mechanism but also to identify photoproducts.

Fenvalerate (**I**) [sumicidin, (*RS*)-α-cyano-3-phenoxybenzyl (*RS*)-2-(4-chlorophenyl)-3-methylbutyrate] is one of the most potent pyrethroid insecticides (*2*), controlling a wide range of insect pests in agricultural fields, public health situations, and animal houses (*3*). The photodegradation profiles of **I** and its insecticidally active 2*S*α*S*-isomer (esfenvalerate) have been investigated in organic solvents, in an aqueous solution, and on soil/clay surfaces (*4*−*6*). Hydration of the α-cyano group and *O*-dephenylation were predominant pathways on these solid surfaces, whereas the unique decarboxylation reaction was observed in solvents, that is, homolytic cleavage of the α-cyanobenzyl carbon−oxygen bond to form radical intermediates being recoupled after release of carbon dioxide within a solvent cage, as illustrated in Scheme 1 of **Figure 1** (*4, 7*). The yield of photoinduced decarboxylation is known to be significantly higher than those for other synthetic pyrethroids possessing the α-cyano 3-phenoxybenzyl moiety such as deltamethrin (*8*) and fenpropathrin (*9*) due to the weak strength of the benzyl carbon−oxygen bond in the excited states calculated by semiempirical molecular orbital calculations (*10*).

Involvement of a radical mechanism for **I** has been demonstrated by identification of radical intermediates using a radical trapping method combined with high-performance liquid chromatography (HPLC), electron spin resonance (ESR), and gas chromatography−mass spectrometry (GC-MS) analyses (*11*). Nitroxides as radical trapping reagents are known to react with carbon-centered radicals such as benzyl at rate constants of 10^7-10^9 M^{-1} s^{-1} to form stable and diamagnetic *O*-alkylhydroxylamines (*12, 13*). Blough et al. have developed a radical trapping technique combined with a highly selective and sensitive HPLC-fluorescence analysis and demonstrated its feasibility in determining the production rates of a hydroxyl radical in a sub-nanomolar level in either aqueous solution (*14*−*16*) or biological systems (*17, 18*). In the present study, this technique was newly applied to detect short-lived free radicals generated in the photolysis of **I**. The aliphatic nitroxide free radical, 3-amino-2,2,5,5-tetramethyl-1-pyrrolidinyloxy free radical (3-AP), was employed to trap the photogenerated benzyl radicals from **I** to form stable and diamagnetic trapping adducts, as shown in Scheme 2 of **Figure 1**. The primary amine group of each resultant adduct was consecutively derivatized with 4-phenylspiro[furan-2(3*H*), 1′-phthalan]-3,3′-dione (fluorescamine, FL) (*19*), leading to an intensely fluorescent product (Scheme 3 of **Figure 1**) through elimination of intramolecular quenching (*20, 21*). We have successfully separated and detected the corresponding fluorescent derivatives from **I** by a reversed-phase HPLC-fluorescence analysis and identified their structures by an liquid chromatography−mass spectrometry (LC-MS). Furthermore, either solvent viscosity or the reactivity of the

* To whom correspondence should be addressed. E-mail: suzukiy16@sc.sumitomo-chem.co.jp.

10.1021/jf802879q CCC: $40.75
Published on Web 11/05/2008

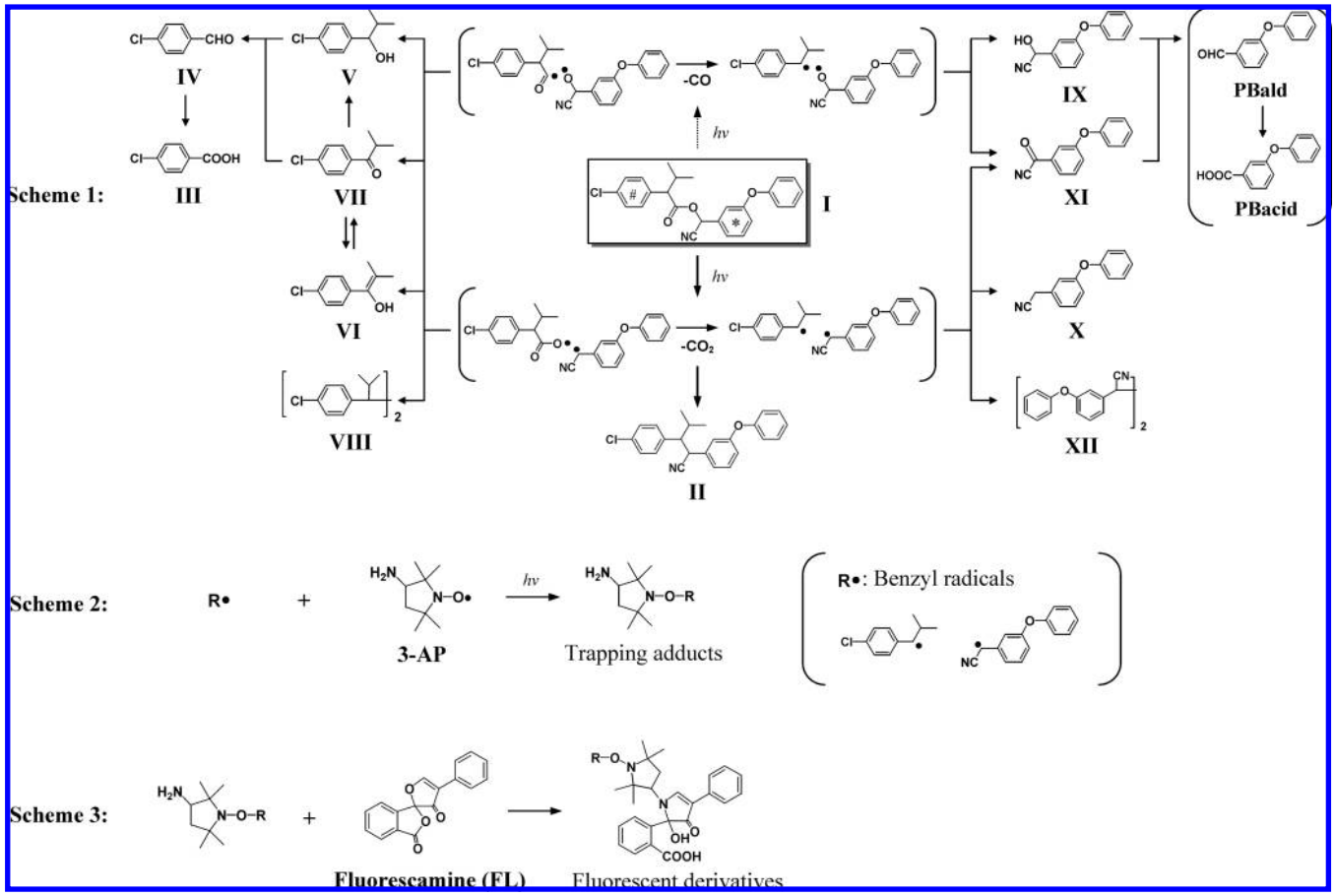

Figure 1. Proposed photolytic pathways and radical-trapping mechanism. ^{14}C-labeled positions of fenvalerate (**I**): *, [PP-^{14}C]-**I**; #, [CP-^{14}C]-**I**.

benzyl radical was found to control the trapping efficiency of radicals through the photodegradation profiles of **I**.

MATERIALS AND METHODS

Chemicals. The two radiolabels of **I**, uniformly labeled with ^{14}C at either the phenoxyphenyl or the chlorophenyl ring, respectively, abbreviated as [PP-^{14}C]-**I** and [CP-^{14}C]-**I** (Scheme 1 of **Figure 1**) were prepared in our laboratory. They were purified prior to use by silica gel thin-layer chromatography ($60F_{254}$; 20 cm × 20 cm, 0.25 mm layer thickness, E. Merck) in *n*-hexane/ethyl acetate (2/1, v/v) and HPLC (YMC-Pack ODS-AM, 300 mm × 10 mm i.d., 5 μm) in acetonitrile/water (4/1, v/v) at 2.0 mL min^{-1}. The specific activities of [PP-^{14}C]-**I** and [CP-^{14}C]-**I** were 11.2 and 10.5 MBq mg^{-1}, respectively, and their radiochemical purities were determined to be greater than 99.8% by HPLC prior to use. The nonradiolabeled **I** with chemical purity of 99.2% was used. The following chemicals were prepared in our laboratory as reference substances for the identification of each degradate: 2-(3-phenoxyphenyl)-3-(4-chlorophenyl)-4-methylpentanenitrile (**II**, decarboxy-fenvalerate), 2-(4-chlorophenyl)-3-methylbutyric acid (CPIA), 1-(4-chlorophenyl)-2-methyl-1-propanol (**V**), 1-(4-chlorophenyl)-2-methyl-1-propanone (**VII**), and dimmer of 1-(4-chlorophenyl)-2-methylpropane (**VIII**). 4-Chlorobenzoic acid (**III**) and 4-chlorobenzaldehyde (**IV**) were purchased from Wako Pure chemicals, Japan. 3-Phenoxybenzaldehyde (PBald), 3-phenoxybenzoic acid (PBacid), 3-phenoxybenzyl cyanide (**X**), and the fluorescent probe FL were purchased from Aldrich Chemical Co., Inc. The radical trapping reagent 3-AP was purchased from Across Organic Inc. Stock solutions of FL (7.2 mM) and 3-AP (24 mM) were prepared daily in acetonitrile, respectively. The borate buffer (10 mM, pH 8) was prepared from Puric MX-II_{AN} water equipped with a G-10 filter (Organo Co., Japan).

Chromatography. HPLC was conducted using a Hitachi L-2130 pump linked in series with an L-2400 UV detector at 254 nm or an L-2480 fluorescence detector and Perkin-Elmer radiochromatography (RI) detector series 610TR equipped with a 500 μL liquid cell, where Ultima-Flo AP (Perkin-Elmer) was utilized as a scintilator. The excitation and emission wavelengths of the fluorescence detector were set at 390 and 490 nm each with a 15 nm band-pass, respectively, on the basis of the reported absorption and fluorescence spectra of an analogous series of FL-derivatized nitroxides (*22*). A Sumipax ODS A-212 column (150 mm × 6 mm i.d., 5 μm, Sumika Chemical Analytical Service Co., Ltd.) was employed for an analytical purpose at a flow rate of 1 mL min^{-1}. The following solvent program was used for typical analyses: 0 min, %A (0.05% formic acid):%B (acetonitrile), 90:10; 0−10 min, linear, 45:55 at 10 min; 10−40 min, linear, 5:95 at 40 min; 40−45 min, isocratic, 5:95 at 45 min. Each ^{14}C peak was identified in HPLC cochromatography by comparing its retention time with those of nonradiolabeled reference standards. Solvent A was changed to 30 mM ammonium acetate (pH 6.98) in analyzing the fluorescence derivative samples of the cholorobenzyl radical adduct to improve resolution of peaks. Typical retention times of **I** and its photodegradates were tabulated in **Table 2**.

Radioassay. Radioactivity in each photolysis test solution was determined in duplicate by mixing each aliquot with 10 mL of Packard Emulsifier Scintillator Plus and analyzed by liquid scintillation counting (LSC) for 5 min with a Packard model 2000CA and 2900TR equipped with an automatic external standard. The background level of radioactivity in LSC was 0.5 Bq, which was subtracted from the disintegrations per minute value of a measured sample.

Spectroscopy. LC-MS in positive and negative ion modes was performed by a Waters ZQ 2000 spectrometer with an ESCi multimode probe, electrospray and atmospheric pressure chemical ionization modes, connected to a Waters Aliance HPLC system. Samples dissolved in acetonitrile were injected using an autosampler at ambient temperature with a flow rate of 0.2 mL min^{-1} using the same gradient system as HPLC analyses. The ultraviolet−visible (UV−vis) absorption spectra of **I** and 3-AP in methanol were obtained using a Shimadzu UV-2550 UV−visible spectrometer in a quartz cuvette (1 cm path length). NMR spectra were measured in $CDCl_3$ by a Varian Mercury 400-BB FT-

NMR spectrometer operating at 400.44 MHz for proton NMR measurement equipped with a 4-Nucleus auto-NMR probe, using tetramethylsilane as an internal standard.

Radical Trapping Study. Approximately a 2.4 mM concentration of each ^{14}C-**I** diluted with nonlabeled standard (0.08−0.09 MBq) was dissolved in 2 mL of *n*-hexane, acetonitrile, methanol, or acetonitrile/water (60/40, v/v). A glass-capped 1 cm quartz cuvette containing each solution was irradiated with a 500 W xenon arc lamp (Ushio Inc., Tokyo) through the UV-cutting filter (UV-29, Toshiba Co., Tokyo) under air at room temperature. For the *n*-hexane solution of [CP-^{14}C]-**I**, radical trapping experiments were also conducted after concisely removing oxygen by gentle bubbling with nitrogen gas for 15 min in an ice−water bath prior to irradiation. For all conditions, the irradiation experiments in the absence of 3-AP or **I** were conducted as controls. The spectral irradiance of xenon arc lamp through the cutoff filter was measured in front of the cell to be approximately 107 W m^{-2} at the wavelengths from 300 to 400 nm by using a USR-40 spectroradiometer (Ushio Inc., Tokyo). After irradiation for 0.5 h, a 5 μL aliquot of each solution was taken for radioassay in duplicate and a 30 μL aliquot was directly subjected to the HPLC-UV-RI analysis. A 300 μL aliquot of each irradiated solution was separately taken in a glass vial, and its pH was adjusted to 8 by adding a 50 μL of the borate buffer. A 100 μL aliquot of FL stock solution was subsequently added to the solution and stirred for 1 min at room temperature. The 40 and 1 μL aliquots of the resulting solution were injected into HPLC-RI and HPLC-fluorescence analyses, respectively. Furthermore, 5 μL portions of the irradiated and derivatized solutions were individually subjected to LC-APCI/ESI-MS analyses for the structural identification.

Photolysis of I. The photodegradation profiles of each labeled **I** in *n*-hexane were investigated in a similar manner with the radical trapping experiment in the absence of 3-AP. After irradiation for 0.5, 1, and 2 h under air or N_2, 5 and 30 μL aliquots of each test solution were subjected to radioassay in duplicate and HPLC-UV-RI analysis, respectively. The chemical identity of major photodegradates was confirmed by the comparison of HPLC retention times and MS spectra with reference substances. Furthermore, the major unknown photodegradates were isolated by HPLC for LC-APCI/ESI-MS and NMR analyses. The spectroscopic data of each isolated component were as follows: **II**, MS (*m*/*z*): 374 ([M − H]$^-$); **III**, MS (*m*/*z*): 155 ([M − H]$^-$); **IV**, MS (*m*/*z*): 141 ([M + H]$^+$), 113 ([M − CO + H]$^+$); **V**, MS (*m*/*z*): 167 ([M − (H$_2$O) + H]$^+$), 125 ([M − OH − CH(CH$_3$)$_2$ + H]$^+$), ^{1}H NMR: δ 7.29−7.32 (m, 2H, Ph-H), 7.24−7.26 (m, 2H, Ph-H), 4.36 (qd, 1H, J = 3.2−3.6 Hz, −C<u>H</u>−OH), 1.92 (m, 1H, J = 6.8 Hz, −C<u>H</u>(CH$_3$)$_2$), 1.85 (d, 1H, J = 3.2 Hz, −O<u>H</u>), 0.97 (d, 3H, J = 6.8 Hz, −CH(C<u>H</u>$_3$)$_2$), 0.80 (d, 3H, J = 6.8 Hz, −CH(C<u>H</u>$_3$)$_2$); **VI**, MS (*m*/*z*): 183 ([M + H]$^+$), 164 ([M − OH + H]$^+$), 141 ([M − C(CH$_3$)$_2$ + H]$^+$); **VII**, MS (*m*/*z*): 183 ([M + H]$^+$), ^{1}H NMR: δ 7.90 (d, 2H, J = 8.4 Hz, Ph-H), 7.44 (d, 2H, J = 8.4 Hz, Ph-H), 3.51 (m, 1H, J = 6.8−7.2 Hz, −C<u>H</u>(CH$_3$)$_2$), 1.20−1.22 (d, 6H, J = 6.8 Hz, −CH(C<u>H</u>$_3$)$_2$); **VIII**, MS (*m*/*z*): 358 ([M + Na]$^+$); **IX**, MS (*m*/*z*): 226 ([M + H]$^+$), 208 ([M − (H$_2$O) + H]$^+$); **X**, MS (*m*/*z*): 210 ([M + H]$^+$), 208 ([M − H]$^-$); **XII**, MS (*m*/*z*): 417 ([M + H]$^+$), ^{1}H NMR: δ 7.35 (m, 6H, Ph-H), 7.15 (t, 2H, J = 7.2 Hz, Ph-H), 7.01−7.06 (m, 4H, Ph-H), 6.95−6.98 (m, 4H, Ph-H), 6.82 (d, 2H, J = 17.6 Hz, Ph-H), 4.20 (2H, d, J = 4.0 Hz, −C<u>H</u>CN−).

RESULTS

Spectroscopy. The UV absorption spectrum of **I** in methanol (**Figure 2**) exhibited weak absorption at 277 nm (ϵ = 2110 M^{-1} cm^{-1}) due to the $\pi-\pi^*$ transition at the phenyl ring with the $n-\pi^*$ character of the carbonyl moiety in good agreement with that reported for 10% acetonitrile solution (*6*). The UV absorption maximum of 3-AP was located at 233 nm (ϵ = 2290 M^{-1} cm^{-1}) with its shoulder extending to wavelengths at >290 nm (ϵ < 100 M^{-1} cm^{-1}), which slightly overlapped with the emission spectrum of the xenon arc lamp through the UV-29 cutoff filter. Because little deterioration of 3-AP was confirmed

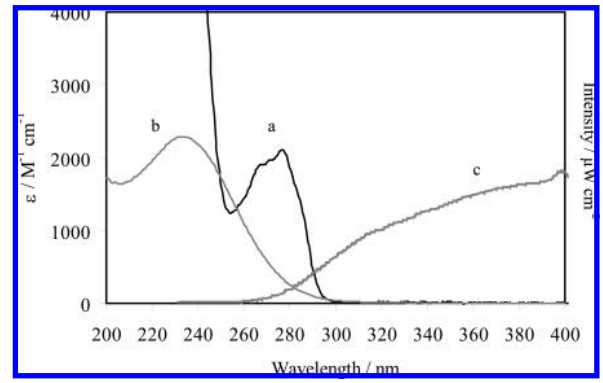

Figure 2. Absorption spectra of **I** (**a**) and 3-AP (**b**) in methanol and spectral irradiance of a 500 W Xe arc lamp (**c**).

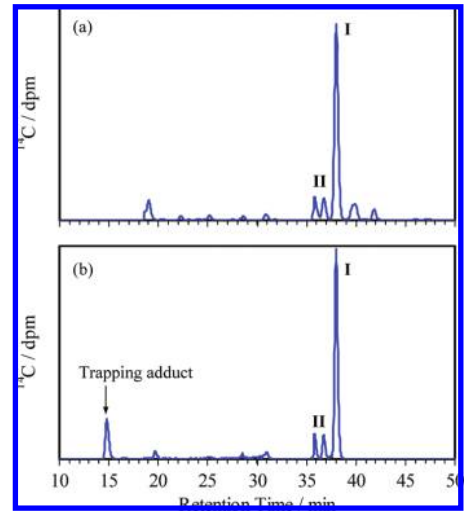

Figure 3. HPLC-RI chromatograms of [PP-^{14}C]-**I** sample in the absence (**a**) or presence (**b**) of 3-AP after 0.5 h of irradiation in *n*-hexane under air.

by HPLC-UV analysis after irradiation for 0.5 h (>98.4% recovery, data not shown), the irradiation condition was found to be appropriate for the radical trapping experiments.

Radical Trapping of I. Figure 3 shows the HPLC-RI chromatograms of the irradiated *n*-hexane solution (0.5 h) treated with [PP-^{14}C]-**I** in the absence (**a**) or presence (**b**) of 3-AP under aerated conditions. In addition to the two peaks corresponding to racemic mixtures of **II**, a new one appeared at approximately 15 min in the presence of 3-AP. The corresponding peak was found to have a molecular weight of 365 as evidenced from at *m*/*z* 366 ([M + H]$^+$), and its chemical structure was assigned to be the phenoxybenzyl adduct trapping with 3-AP (Scheme 2). These results strongly indicated that 3-AP efficiently trapped the phenoxybenzyl radical generated via homolytic cleavage of ester linkage of **I** even in the presence of oxygen. The irradiated solution derivatized with FL was analyzed by HPLC-RI and HPLC-fluorescence detectors, as shown in **Figure 4a**,**b**, respectively. The 15 min peak assigned to be the phenoxybenzyl trapping adduct completely disappeared with a concomitant appearance of a relatively broad peak around 32 min in the HPLC-RI chromatogram, and an intense peak with high fluorescence was observed at the same retention time in the HPLC-fluorescence one. The LC-APCI-MS spectrum of this peak showed a molecular ion at *m*/*z* 644 ([M + H]$^+$) with its fragment at *m*/*z* 436 ([M − phenoxybenyl + H]$^+$), indicating that its chemical structure corresponds to a fluorescent derivative with the 3-phenoxybenzyl trapping adduct (MW 643). Similarly, in the case of radical trapping experiments using [CP-^{14}C]-**I**, a

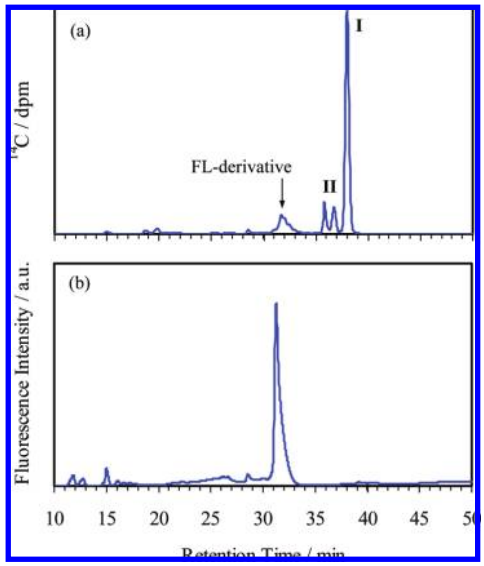

Figure 4. HPLC-RI (**a**) and HPLC-fluorescence (**b**) chromatograms of [PP-^{14}C]-**I** sample derivatized with FL after 0.5 h of irradiation in *n*-hexane under air.

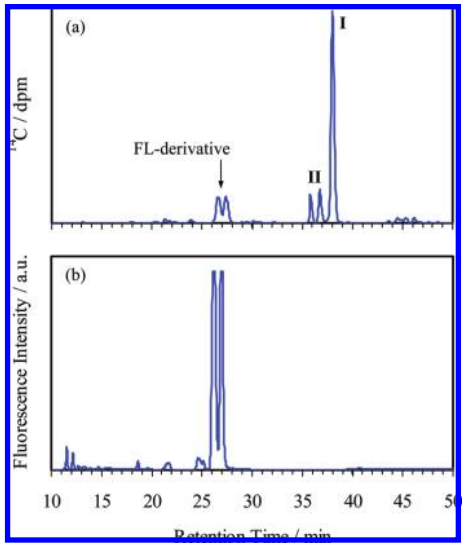

Figure 5. HPLC-RI (**a**) and HPLC-fluorescence (**b**) chromatograms of [CP-^{14}C]-**I** sample derivatized with FL after 0.5 h of irradiation in *n*-hexane under N_2.

new peak was observed at 16 min under N_2 but not detected under aerated conditions (data not shown). Its chemical structure was assigned to be the chlorobenzyl trapping adduct with its molecular weight of 324, as evidenced from the MS spectrum at *m/z* 325 ($[M + H]^+$). The generated trapping adduct was completely derivatized with FL to exhibit two peaks at 26 and 27 min in HPLC-RI and HPLC-fluorescence analyses, as shown in **Figure 5a**,**b**. These corresponding peaks have the same molecular weight of 602 as evidenced from the LC-ESI-MS spectrum at *m/z* 603 ($[M + H]^+$) with its fragments at *m/z* 436 ($[M -$ chlorobenzyl $+ H]^+$) and 325 ($[M -$ FL moiety $+ H]^+$), indicating that the formation of racemic fluorescence derivatives from the chlorobenzyl trapping adducts. The derivatization with FL proceeded in 89.9−97.8% yield by radioanalysis.

Trapping Efficiency of Phenoxybenzyl Radical. Solvent viscosity (η) is known to be one of the most important parameters to control an efficiency in recombination of geminate radicals in solvent cage (*23*). To investigate the trapping efficiency of the relatively stable phenoxybenzyl radical escaped from a solvent cage by diffusion, the irradiation experiments in acetonitrile, methanol, or acetonitrile/water (60/40, v/v) solution of [PP-^{14}C]-**I** with 3-AP was similarly conducted under air. After 0.5 h of exposure, the phenoxybenzyl trapping adduct with 3-AP eluting at 15 min was observed in the HPLC-RI chromatograms with quite different amounts depending on solvent: 13.7% AR (applied radioactivity), *n*-hexane; 11.3% AR, acetonitrile; 6.6% AR, methanol; and 2.0% AR, acetonitrile/water (60/40), as summarized in **Table 1**. Simultaneously, the amounts of **I** remaining in each test solution decreased to 63.6−77.1% AR with a concomitant formation of **II** increasing up to 11.0−17.9% AR as racemic mixtures. The reciprocals of each solvent viscosity at 20−30 °C (*24, 25*) are plotted against the % AR ratio of the trapping adduct to the total amounts of **II** and the trapping adduct, as shown in **Figure 6**. The ratio of the adduct via trapping the phenoxybenzyl radical with 3-AP was found to linearly increase with the solvent fluidity (η^{-1}).

Table 1. Trapping Efficiency of the Phenoxybenzyl Radical in Each Solvent

	% of the applied ^{14}C after 0.5 h of irradiation			
	solvents			
compd	*n*-hexane	acetonitrile	methanol	acetonitrile/water (60/40, v/v)
I	63.6	72.5	68.4	77.1
II	14.2	11.0	15.7	17.9
trapping adduct	13.7	11.3	6.6	2.0
others	11.0	3.7	11.7	8.5
total	102.5	98.5	102.4	105.5

Photolysis of I. On irradiation with a xenon lamp for 2 h, **I** underwent rapid photodegradation with significant formation of **II** as reported previously (*4*). The formation of **II** under N_2 (47.6−54.8% AR) was found to be accelerated relative to that under air (26.9−33.3% AR) after 2 h of exposure, as summarized in **Table 2**. From [CP-^{14}C]-**I**, **V** and **VII** were formed as the major photodegradates under air, each amounting up to 10.9 and 23.4% AR after 2 h, respectively. In contrast, a significant amount of **VIII** (17.4% AR after 2 h) was detected under N_2, accompanied with 3−7-fold less amounts of **V** and **VII**. The formation of **III**, **IV**, and **VI**, suspected as subsequent degradates or tautomer of **V** and **VII**, were also retarded. One of the major degradates in aqueous solution CPIA (*5*) was not detected throughout the experiments due to the apolar environment. In the case of treatment with [PP-^{14}C]-**I**, four degradates in addition to **II** were characterized by LC-MS and/or NMR analyses. Although the formation of PBald and PBacid was not detected, their precursor **IX** was detected as the major photodegradate under both air and N_2, amounting to 20.8−35.3% AR after 2 h. The amounts of **X** and **XII** under N_2 (4.9% and 4.2% AR after 2 h) were slightly higher than those under air, whereas the formation of **XI** moderately retarded from 5.3% AR under air to 1.9% AR under N_2. Although **XI** could not be isolated due to its instability, the mass at *m/z* 222 ($[M - H]^-$) with its fragment at *m/z* 169 ($[M - (CO-CN)]^-$) in the LC-ESI-MS analysis (negative ion mode) supports the 3-phenoxybenzoyl cyanide. On the basis of these results, the main photolytic pathways of **I** in *n*-hexane are similar to those reported (*4*) and are proposed in Scheme 1 of **Figure 1**.

DISCUSSION

One of the most important findings in this study was the convenient fluorescence detection of the benzyl radicals of **I** trapped by 3-AP through photodegradation, together with identification of their structures by LC-MS analysis. Fluores-

Table 2. Photodegradation of **I** in *n*-Hexane under Air and N_2[a]

		% of the applied ^{14}C							
		[CP-^{14}C]-**I**				[PP-^{14}C]-**I**			
		air		N_2		air		N_2	
compd	HPLC retention time (min)	0.5 h	2 h	0.5 h	2 h	0.5 h	2 h	0.5 h	2 h
I	38.0	64.7	14.1	57.5	7.0	59.9	12.7	60.7	9.4
II	35.8, 36.8[b]	15.9	33.3	24.7	54.8	15.0	26.9	19.1	47.6
III	16.0	ND	2.8	ND	ND	−	−	−	−
IV	17.9	ND	2.9	ND	2.1	−	−	−	−
V	20.5	2.6	10.9	0.4	3.4	−	−	−	−
VI	21.3	5.8	4.8	0.4	2.2	−	−	−	−
VII	23.9	3.8	23.4	0.4	3.3	−	−	−	−
VIII	46.6,48.2[b]	ND	ND	8.8	17.4	−	−	−	−
IX	18−19	−	−	−	−	7.9	35.3	3.3	20.8
X	21.8	−	−	−	−	ND	ND	0.5	4.9
XI	25.3	−	−	−	−	1.5	5.3	0.6	1.9
XII	31.0	−	−	−	−	1.8	1.6	5.6	4.2
others		5.8	5.9	6.4	13.9	14.9	13.6	11.2	10.1
total		98.6	98.1	98.6	104.1	101.0	95.4	101.0	98.9

[a] ND, not detected; −, not formed when using the corresponding radiolabeled one. [b] Two retention times of **II** and **VIII** represented the separation of their diastereomers.

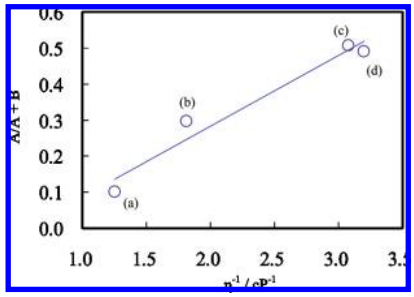

Figure 6. Relationship between the solvent fluidity and the radical-trapping efficiency. η: solvent viscosity. **(a)** acetonitrile/water (60/40,v/v), **(b)** methanol, **(c)** acetonitrile, **(d)** *n*-hexane. A: % AR of the 3-phenoxybenzyl trapping adduct with 3-AP after 0.5 h of irridation. B: % AR of **II** after 0.5 h of irridation.

cence bands were not observed in the absence of **I** or 3-AP because fluorescence is emitted only after conversion of a paramagnetic radical species to a diamagnetic one by derivatization to the FL-nitroxide trapping adduct due to inhibition of intramolecular quenching (*20, 21*). Holmstead et al. have also proposed another type of photoinduced cleavage at the carbonylcarbon−benzyloxygen bond (*4*), but this pathway was considered to be minor based on much more greater of **II**, **X**, and **XII** under N_2 characteristic of cleavage of the benzylcarbon−oxygen bond (**Table 2**). Because nitroxide compounds are known to rapidly react with carbon-centered radicals but not with most oxygen-centered radicals (*12, 13*), the cyanohydrin type radical generated via this minor pathway is unlikely to be efficiently trapped by the present technique. Assuming that the limit of detection is 1/10 of the corresponding peak heights in the HPLC-fluorescence chromatograms as shown in **Figures 4b** and **5b**, 0.02−0.03 nmol per 1 μL injection of the FL-nitroxide trapping adduct derivatized from each benzyl radical may be detected in the current HPLC-fluorescence analysis.

When the phenoxybenzyl radical was trapped by 3-AP under aerated conditions, significant formation of **II** via recombination of geminate radicals after release of CO_2 was still observed in each solvent (**Table 1** and **Figure 3**), indicating that the escape of these radicals from the solvent cage by diffusion (radical-trapping) was competitive with recombination of the cage pairs. The trapping efficiency of the phenoxybenzyl radical was found to vary linearly with the inverse of solvent viscosity (**Figure 6**). This correlation is consistent with the Noyes model, where the formation ratio of cage pairs depends on diffusion of radical species in relation to the solvent viscosity (*23*). The trapping efficiency of the phenoxybenzyl radical increased with solvent fluidity, and *n*-hexane was considered to be the most appropriate solvent. Although facile trapping of the phenoxybenzyl radical was observed even in the presence of oxygen, the chlorobenzyl radical was only efficiently trapped under N_2. These findings suggested that the trapping capability of each photogenerated benzyl radical by 3-AP was significantly dependent on its reactivity toward oxygen. The reaction rates of resonance-stabilized carbon-centered radicals with molecular oxygen are similar to those of nonstabilized ones with rate constants of $\sim 10^9-10^{10}$ M^{-1} s^{-1} (*26*), whereas nitrile and nitro groups attached to a radical center are known to significantly attenuate the rate constants to below 5×10^3 M^{-1} s^{-1} due to spin delocalization on the nitrogen atom (*27, 28*). These facts apparently reflected the significant differences in the product distribution between the air and the N_2 atmosphere for [CP-^{14}C]-**I**, as compared with [PP-^{14}C]-I (**Table 2**). A significant decrease of **V** and **VII** formed via oxidation of the chlorobenzyl radical was found under N_2 with a concomitant increase of the dimerization product **VIII**. Although a similar tendency was observed in the product distribution originating from the phenoxybenzyl radical, **IX** was consistently detected as the major photodegradate but with lesser amount of the corresponding oxidized compound **XI** and greater formation of the dimer **XII** under N_2. Incidentally, the formation of **X** via hydrogen abstraction from the solvent by the phenoxybenzyl radical was observed under N_2 but only as a minor product due to its lower reactivity with the hydrogen atom (*29*).

In conclusion, we investigated a novel approach to detect short-lived free radicals by combining a radical trapping technique with a highly sensitive and selective reversed-phase HPLC-fluorescence analysis. It was clearly demonstrated that the photogenerated benzyl radicals from **I** were trapped by nitroxide compound under N_2, especially for α-cyano-3-phenoxybenzyl radical even under aeration. The instantaneous reaction of these trapping adducts with FL proceeded quantitatively to form the highly fluorescent products suitable for reversed-phase HPLC analysis with a fluorescence detector, and the chemical structures of the corresponding fluorescence derivatives were successfully identified by LC-MS. This is the first time that a fluorescence spectroscopic method has been

coupled with HPLC and LC-MS to detect short-lived radical intermediates from photolysis of a pesticide. This approach can be used directly to study other pesticides.

LITERATURE CITED

(1) Tsao, R.; Eto, M. Effect of some natural photosensitizers of photolysis of some pesticides. In *Aquatic and Surface Photochemistry*; Helz, G. R., Zepp, R. G., Crosby, D. G., Eds.; Lewis Publishers: Boca Raton, FL, 1994; pp 163−171.

(2) Matsuo, T.; Itaya, N.; Mizutani, T.; Ohno, N.; Fujimoto, K.; Okuno, Y.; Yoshioka, H. 3-Phenoxy-α-cyano benzyl esters, the most potent synthetic pyrethroids. *Agric. Biol. Chem.* **1976**, *40*, 247–249.

(3) Robert, T.; Huston, D. Metabolic Pathways of Agrochemicals, Part Two: Insecticides and Fungicides; The Royal Society of Chemistry: Cambridge, United Kingdom, 1998; pp 659−666.

(4) Holmstead, R. L.; Fullmer, D. G.; Ruzo, L. O. Pyrethroid photodecomposition: Pydrin. *J. Agric. Food Chem.* **1978**, *26*, 954–959.

(5) Mikami, N.; Takahashi, N.; Hayashi, K.; Miyamoto, J. Photodegradation of Fenvalerate (Sumicidin®) in water and on soil surface. *J. Pesticide. Sci.* **1980**, *5*, 225–236.

(6) Katagi, T. Photodegradation of the pyrethroid insecticide esfenvalerate on soil, clay minerals, and humic acid surfaces. *J. Agric. Food Chem.* **1991**, *39*, 1351–1356.

(7) Holmstead, R. L.; Fullmer, D. G. Photodecarboxylation of cyanohydrin esters. Models for pyrethroid photodecomposition. *J. Agric. Food Chem.* **1977**, *25*, 56–58.

(8) Ruzo, L. O.; Holmstead, R. L.; Casida, J. E. Pyrethroid photodecomposition: Decamethrin. *J. Agric. Food Chem.* **1977**, *25*, 1385–1394.

(9) Takahashi, N.; Mikami, N.; Yamada, H.; Miyamoto, J. Photodegradation of the pyrethroid insecticide fenpropathrin in water, on soil and on plant foliage. *Pestic. Sci.* **1985**, *16*, 119–131.

(10) Katagi, T.; Mikami, N.; Matsuda, T.; Miyamoto, J. Molecular orbital and experimental studies on the photoinduced decarboxylation of pyrethroid model esters. *J. Chem. Soc. Perkin Trans. II* **1989**, 779–782.

(11) Mikami, N.; Takahashi, N.; Yamada, H.; Miyamoto, J. Separation and identification of short-lived free radicals formed by photolysis of the pyrethroid insecticide fenvalerate. *Pestic. Sci.* **1985**, *16*, 101–112.

(12) Beckwith, A. L. J.; Bowry, V. W.; Ingold, K. U. Kinetics of nitroxide radical trapping. 1. Solvent effects. *J. Am. Chem. Soc.* **1992**, *114*, 4983–4992.

(13) Bowry, V. W.; Ingold, K. U. Kinetics of nitroxide radical trapping. 2. Structural effects. *J. Am. Chem. Soc.* **1992**, *114*, 4992–4996.

(14) Kieber, D. J.; Blough, N. V. Fluorescence detection of carbon-centered radicals in aqueous solution. *Free Radical Res. Commun.* **1990**, *10* (1−2), 109–117.

(15) Kieber, D. J.; Blough, N. V. Determination of carbon-centered radicals in aqueous solution by liquid chromatography with fluorescence detection. *Anal. Chem.* **1990**, *62*, 2275–2283.

(16) Vaughan, P. P.; Blough, N. V. Photochemical formation of hydroxyl radical by constituents of natural waters. *Environ. Sci. Technol.* **1998**, *32*, 2947–2953.

(17) Li, B.; Gutierrez, P. L.; Blough, N. V. Trace determination of hydroxyl radical in biological systems. *Anal. Chem.* **1997**, *69*, 4295–4302.

(18) Li, B.; Gutierrez, P. L.; Amstad, P.; Blough, N. V. Hydroxyl radical production by mouse epidermal cell lines in the presence of quinone anti-cancer compounds. *Chem. Res. Toxicol.* **1999**, *12*, 1042–1049.

(19) Udenfriend, S.; Stein, S.; Böhlen, P; Dairman, W.; Leimgruber, W; Weigele, M. Fluorescamine: A reagent for assay of amino acids, peptides, proteins, and primary amines in the picomole range. *Science* **1972**, *178*, 871–872.

(20) Blough, N. V.; Simpson, D. J. Chemically mediated fluorescence yield switching in nitroxide-fluorophore adducts: Optical sensors of radical/redox reactions. *J. Am. Chem. Soc.* **1988**, *110*, 1915–1917.

(21) Gerlock, J. L.; Zacmanidis, P. J.; Bauer, D. R.; Simpson, D. J.; Blough, N. V.; Salmeen, I. T. Fluorescence detection of free radicals by nitroxide scavenging. *Free Radical Res. Commun.* **1990**, *10* (1−2), 119–121.

(22) Herbelin, S. E.; Blough, N. V. Intramolecular quenching of excited singlet states in a series of fluorescamine-derivatized nitroxides. *J. Phys. Chem. B* **1998**, *102*, 8170–8176.

(23) Koenig, T.; Fisher, H. In *Free Radicals*; Kochi, J. K., Ed.; Wiley: New York, 1973; Vol. 1, pp 157−189.

(24) Riddick, J. A.; Bunger, W. B. In *Organic Solvents, Physical Properties and Methods of Purification*, 3rd ed.; Wiley-Interscience: New York, 1970; Vol. 2.

(25) Timmermans, J. In *The Physico-chemical Constants of Binary Systems in Concentrated Solutions, Systems with Inorganic + Organic or Inorganic Compounds*; Interscience Publishers, Inc.: New York, 1960; Vol. 4.

(26) Maillard, B.; Ingold, K. U.; Scaiano, J. C. Rate constants for the reactions of free radicals with oxygen in solution. *J. Am. Chem. Soc.* **1983**, *105*, 5095–5099.

(27) Font-Sanchis, E.; Aliaga, C.; Focsaneanu, K-S.; Scaiano, J. C. Greatly attenuated reactivity of nitrile-derivatived carbon-centered radicals toward oxygen. *Chem. Commun.* **2002**, 1576–1577.

(28) Font-Sanchis, E.; Aliaga, C.; Cornejo, R.; Scaiano, J. C. Reactivity toward oxygen of isobenzofuranyl radicals: Effect of nitro group substitution. *Org. Lett.* **2003**, *5*, 1515–1518.

(29) Sanjuán, A.; Aguirre, G.; Alvaro, M.; García, H.; Scaiano, J. C.; Chrétien, M. N.; Focsaneanu, K.-S. Product studies and laser flash photolysis of direct and 2,4,6-triphenylpyrylium-zeolite Y photocatalyzed degradation of fenvalerate. *Photochem. Photobiol. Sci.* **2002**, *1*, 955–959.

Received for review June 26, 2008. Accepted September 26, 2008.

JF802879Q